Ultra-thin EBG backed flexible antenna for 24 GHz ISM band WBAN

Mubasher Ali
John C. Batchelor
School of Engineering
University of Kent
Canterbury, United Kingdom
ma954@kent.ac.uk

Irfan Ullah
Department of Electronic and Computer Science
University of Southampton
Southampton, United Kingdom

Nathan J. Gomes
School of Engineering, University of Kent
Department of Electronic and Electrical Engineering, UCL
United Kingdom.

***Abstract*—An ultra-thin, electromagnetic bandgap (EBG) backed antenna is presented for 24 GHz ISM band wearable applications. The antenna is a slotted bow-tie, with an overall dimension of $0.91\lambda_0 \times 0.84\lambda_0 \times 0.01\lambda_0$, backed by a 5×5 element $0.01\lambda_0$ thick EBG structure; it is manufactured on a flexible substrate (ε_r = 2.2). The performance of the EBG-backed antenna in terms of reflection coefficient and free-space radiation patterns is investigated in scenarios with and without structural bending. It is shown that the integration of the EBG enhances the antenna's front-lobe gain by 2.63 dBi, decreases back-lobe radiation by 12.2 dB, and decreases the specific absorption rate (SAR (1 g)) from > 28 W/kg to <1.93 W/kg, significantly reducing potential harm to the human body. Furthermore, the results show the performance of the EBG-backed antenna is highly insensitive to body proximity, and that its performance is preserved when bent along the either axis.**

***Index Terms*—Slot antenna, EBG, AMC, ultra-thin, 24 GHz ISM, WBAN**

I. Introduction

Lately, wireless communication networks have been driven towards the mm-wave frequencies due to large amount of unused bandwidth, lower latency, and capability to achieve high throughput. Therefore, Millimeter wave frequencies have attracted the wireless body area network community as it offers great potential to further improve health care and remote sensing application [1-3]. The mm-wave spectrum provides plenty of advantages like reduced interference due to uncongested unlicensed bandwidth, compact devices, and large data rates[4]. Recently, A 24 GHz ISM band Yagi Uda antenna has been developed on a flexible substrate using inkjet printing [5]. Moreover, A 60 GHz wearable end-fire antenna has been proposed for on-body communication [6]. However, these wearable antennas have high backward radiation which cause a potential hazard to the human body. Millimeter waves have very short wavelengths, therefore penetration depth of mm-waves frequencies is restricted to 1 mm. Due to very close proximity of human skin tissue with antenna further reduces the performance of the antenna [7]. To overcome this challenge, good isolation is required between the human skin and the antenna. An electromagnetic bandgap (EBG) structure is widely used to suppress the surface waves and back lobe radiations of the antenna. A square-shaped EBG printed on textile material has been proposed for a 26 GHz antenna which enhances the gain by 2.52 dBi [8].

In this Paper, low profile thin layered antenna integrated with a dual split square ring EBG structure with the thickness of $0.02\lambda_0$ is presented. The proposed antenna is a slotted bow-tie, backed by an array of 5×5 cell EBG structure demonstrating required phase reflection at 24 GHz, which substantially reduces the backward radiation of the antenna. Table 1 presents the comparisons of different features of the proposed antenna with previously published K band EBG integrated antennas. The proposed antenna is the thinnest and smallest in size. This antenna covers 24GHz ISM band when attached directly to the skin, and shows a minimal shift in S11 while bending, and a significant decrease in SAR percentage. The rest of the paper is organized as follows: In Section II, the design of the Bow-tie

TABLE I
COMPARISON WITH PREVIOUSLY PUBLISHED K BAND EBG ANTENNAS

Ref	Frequency GHz	Dimension mm^2	Thickness (mm)	Gain dBi	On-body S11 BW(MHz/%)	S11 shift MHz / radius mm	Gain/bending radius mm	Reduction in SAR %
Proposed	**24**	**(1.29 ×1.29) λ_0**	**$0.02\lambda_0$**	**5.5**	**620 / 2.58%**	**~80 /30**	**1.5 dBi / 15**	**93%**
[9]	26	(2.79×1.91) λ_0	$0.032\lambda_0$	8.65	600/2.3%	~400 /30	NA	69.9%
[10]	28	(2.67×3.14) λ_0	$0.065\lambda_0$	7.9	10GHz/40%	~1500/30	NA	NA
[11]	24	(2.16×2.16) λ_0	$0.05\lambda_0$	6	~720 / 3%	~400 /60	*5.36dBi/60	NA
[12]	28	(1.9 ×1.9) λ_0	$0.14\lambda_0$	5	** 950/3.3%	NA	NA	NA

*Simulated gain when bent along 60 mm radius cylinder
** Free space Impedance Bandwidth

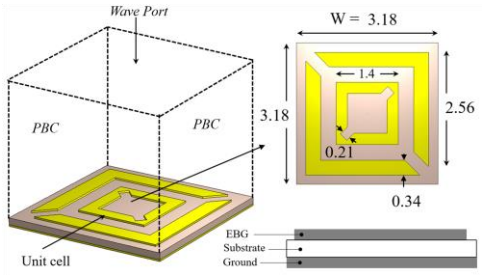

Fig. 1. EBG geometry

slot antenna with EBG structure. In Section III, Experimental and simulation results of the prototyped antenna in terms of the radiations pattern, free space and on-body reflection coefficient S_{11}, structural deformation and SAR.

II. Design of Antenna with EBG Structure

A. EBG Geometry

A dual split square ring resonator based unit cell of $Area = 3.18 \times 3.18\, mm^2$ on a rogers 5880 dielectric material ($\varepsilon_r = 2.2$) and thickness of 127 um over a ground plane is used as shown in Fig. 1. The unit cell was simulated in CST Microwave Studio using periodic boundary conditions (PBCs) and further optimized to obtain the required phase reflection response at 24.125 GHz. This geometry of outer and inner split square ring resonator with coupling gaps on two corners provides 0° phase shift from reflected wave and behaves as an artificial magnetic conductor (AMC).

B. Antenna Design and Integration with EBG

The dimension and geometry of the fabricated co-planar waveguide (CPW) fed bow-tie slot antenna is presented in Fig. 2(a).

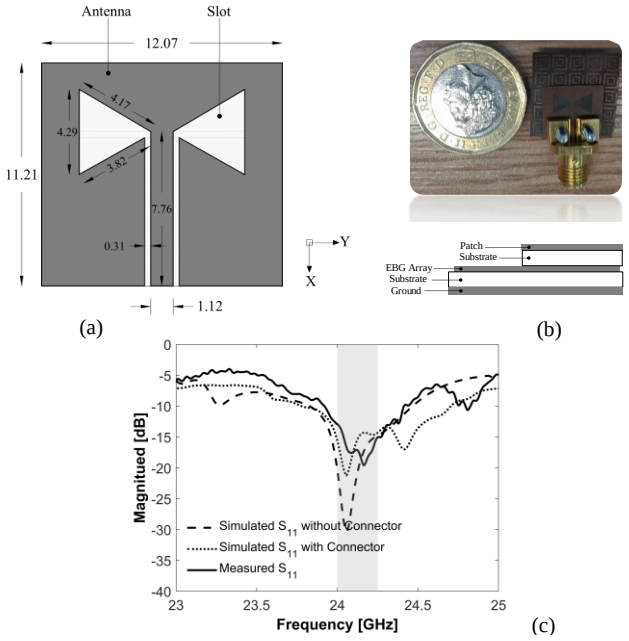

Fig. 2. (a) Bow-tie slot antenna geometry, (b) integration of EBG with antenna, (c) return loss of simulated EBG backed antenna with and without connector and measured S_{11}.

The prototype antenna construction is straightforward because it has a single metallization layer and ungrounded CPW feeding is a suitable option. However, grounded CPW feeding is chosen when the EBG array is attached underneath the antenna as the EBG has a ground plane. The Time-domain solver of CST studio was used to model and simulate the full EBG-backed antenna structure with a 50 ohm SMA connector. Modeling the SMA connector improves the comparison of simulation and measurement results. The chemical etching technique was used in prototyping and fabrication. The dimension of the resultant antenna is $16.19 \times 16.19 \times 0.254\ mm^3$ and the configuration of the antenna structure is shown in Fig. 2(b), where the EBG-backed antenna has edge mount integration with a connector and no air gap between the antenna and EBG. This configuration of the antenna increases its suitability for wearing on the surface of the human body and easy integration with the connector.

III. Results and Discussions

A. Free Space performance Evaluation

The EBG backed antenna was tested in-house, and the measured reflection parameters taken with a 40 GHz VNA (HP 8722ES) are compared with simulation in Fig. 2(c) which indicates the effect of the SMA connector. S_{11}values are less than -10 dB in the desired band, and the measured S_{11} of the EBG backed antenna is around -17 dB in the ISM band (24 - 24.250 GHz).

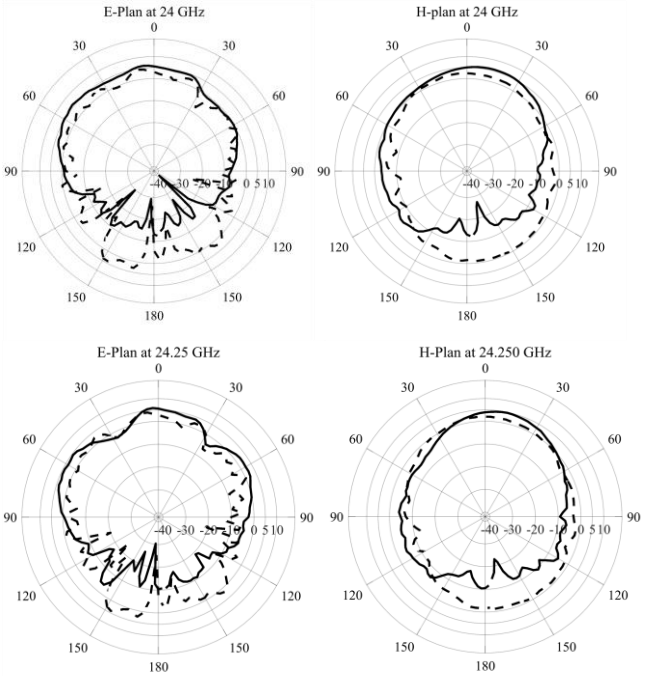

Fig. 3. Measured radiation polar plots of bow-tie slot antenna with EBG/AMC (bold solid-line) and without EBG/AMC (dash-line) at 24, and 24.250 GHz

Fig. 3 shows the measured E- and H-plane patterns. A bold solid line represents a radiation pattern with EBG and the dashed line represents without EBG pattern. After integration of the EBG structure with antenna, backward radiation is

reduced by 12.2 dB at 24 GHz and 10.5 dB at 24.250 GHz, whereas the realized gain increases by 2.63dBi to 5.5 dBi and 2.5 dBi to 4.8 dBi at 24 GHz and 24.25 GHz, respectively. The result shows the significance of the EBG structure in suppressing the back lobe radiations which are directed toward the human body.

B. Structural bending analysis

In on-body reflection response measurements, antenna positions are relatively flat as shown in Fig.6. However, the human body has several curved surfaces which might cause some structural deformation of the antenna. Therefore, a further investigation was performed into the capability to bear structural bending while retaining comparable reflection and radiation performance. Fig. 5 shows the S_{11} measurements of the antenna while bent along the X- and Y-axis with 15 and 30 mm radii of curvature. A slight shift in center frequency is observed when bent on a 30 mm radius cylinder along the X- and Y-axis. However, a larger shift is observed when bent on a 15 mm radius cylinder along the X- and Y-axis but the S11 value remains below -10 dB at 24.125 GHz.

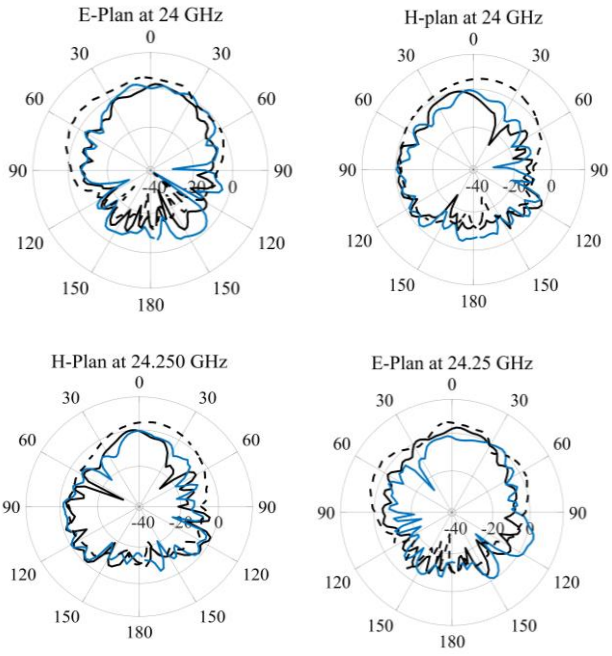

Fig. 4. Measured radiation polar plots of EBG backed antenna when bent on 15 mm radius cylinder along X-axis (black solid-line), Y-axis (blue solid-line) and without bent (dash-line) at 24, and 24.250 GHz.

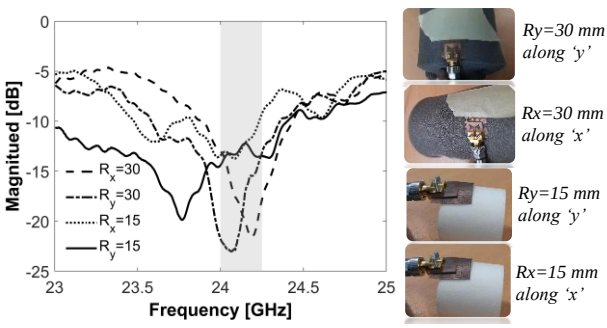

Fig. 5. Reflection Coefficient of the EBG backed antenna when bent along "Y" and "X"

Furthermore, the radiation pattern of the EBG-backed antenna under bending scenario (for Rx, Ry = 15 mm along the y-axis and x-axis) is reported in Fig. 4. The results show the directivity is maintained around 1.5 dBi while bent at Rx, Ry = 15 mm, although the reflection coefficients at Ry = 15mm are slightly detuned from the desired band.

C. SAR and body loading effects

To further investigate the body-loading performance of the prototype antenna, S_{11} measurements were performed on a male volunteer (who was 178 cm in height and weighed 61 kg) at different positions such as chest, finger, forehead, hand, and wrist. The on-body S_{11} measured curves are presented in Fig 6(a). Due to varied dielectric constant values and capacitive behavior of different human tissues, there are differences in the S11 curves measured in different positions.

Therefore, without an EBG, the structure is highly lossy with significant energy dissipated in the human tissues. All the reflection curves are detuned even though measured S_{11} was at < -10 dB over the desired 24 GHz ISM band apart from the wrist. After integration of the EBG structure with the antenna as shown in Fig. 6(b), the reflection response of the structure is tuned for the 24GHz ISM band for all mounting sites. The proposed prototype covers only the 24 GHz ISM band and reduces unwanted wideband absorption of EM energy on human tissues.

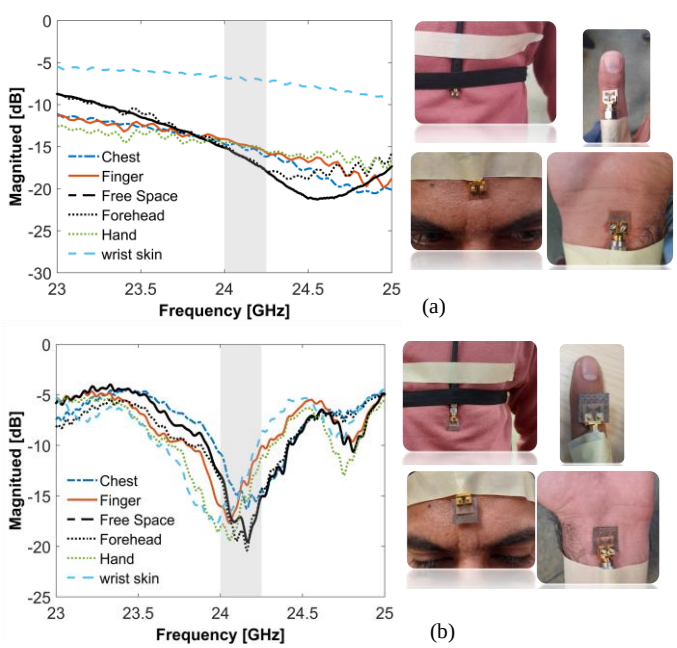

Fig. 6. Measured reflection coefficients of antenna on human body (a) without EBG (b) with EBG

The gap between the antenna aperture and the skin layers is 3 mm in both with and without EBG scenarios. Dielectric properties of both dry and wet human tissue layers are obtained from the Italian National Research Council's website[9]. Relative permittivity $\boldsymbol{\varepsilon_r}$ of dry and wet skin are 18.993 and 20.98, respectively. In CST MWS, the IEEE/IEC 62704-1 averaging method is used for SAR calculation for 1g of tissue volume and Fig. 7 presents the SAR distribution when EBG is

and is not attached to the antenna. The maximum SAR values were 1.93 W/kg and 28.1 W/kg at 100 mW input power, respectively. Hence, the EBG shield reduces 93% of the radiation absorption rate compared to direct exposure from the antenna.

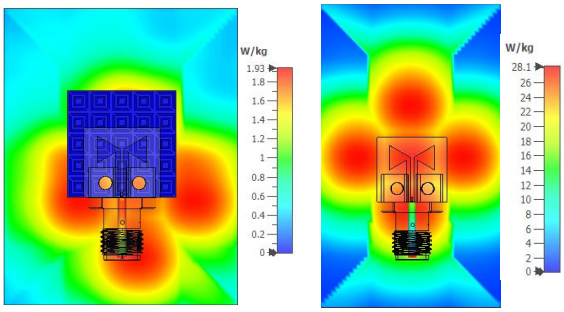

(a) (b)

Fig. 7. SAR distribution of prototype antenna (a) with EBG (b) without EBG

IV. CONCLUSION

In this paper, a low profile thin layered split square ring EBG structure is presented at 24 GHz ISM band. A 5 × 5 element EBG array is investigated beneath a bow-tie slot antenna. This antenna is the thinnest ($0.02\lambda_0$) EBG-backed antenna reported in the K band according to the authors' knowledge. Radiation measurements in the anechoic chamber show an increase in the gain by 2.6 dBi and in the front-to-back ratio by 14.83 dB. High insensitivity to body proximity is observed from the on-body S11 performance of EBG backed antenna. Furthermore, insignificant variation in bandwidth and center frequency is noticed in the results when the proposed antenna is bent over a curve of 30 and 15 mm. Also, measurements of the radiation patterns in bending scenarios show gain and directivity are not significantly altered. Finally, the SAR investigation in CST studio shows a 93% decrease in absorption rate because of the EBG shield under the 100mW input power. The proposed antenna performance demonstrates its suitability for 24 GHz ISM band wearable applications.

REFERENCES

[1] N. F. M. Aun, P. J. Soh, A. A. Al-Hadi, M. F. Jamlos, G. A. E. Vandenbosch, and D. Schreurs, ''Revolutionizing wearables for 5G: 5G technologies: Recent developments and future perspectives for wearable devices and antennas,'' in *IEEE Microw. Mag.*, vol. 18, no. 3, pp. 108–124, May 2017.

[2] Ali, M., Zafar, J., Zafar, H., O'Halloran, M. and Sharif, F., 2019. Multiband ultra-thin flexible on-body transceivers for wearable health informatics. *Australasian physical & engineering sciences in medicine*, 42(1), pp. 53-63.

[3] Arif, A., Zubair, M., Ali, M., Khan, M. U. and Mehmood, M.Q., 2019. "A compact, low-profile fractal antenna for wearable on-body WBAN applications," *IEEE Antennas and Wireless Propag. Lett.*, vol. 18, no. 5, pp. 981-985, May 2019.

[4] H. Attia, M. L. Abdelghani, and T. A. Denidni, "Wideband and high-gain millimeter-wave antenna based on FSS Fabry-Perot cavity," *IEEE Trans. Antennas Propag.*, vol. 65, no. 10, pp. 5589–5594, Oct. 2017.

[5] B. K. Tehrani, B. S. Cook, and M. M. Tentzeris, "Inkjet printing of multilayer millimeter-wave Yagi-Uda antennas on flexible substrates," *IEEE Antennas Wireless Propag. Lett.*, vol. 15, pp. 143–146, 2016.

[6] N. Chahat, M. Zhadobov, L. Le Coq, and R. Sauleau, "Wearable endfire textile antenna for on-body communications at 60 GHz," *IEEE Antennas Wireless Propag. Lett.*, vol. 11, pp. 799–802, 2012.

[7] Tayari, K., Werfelli, H., Chaoui, M., Ghariani, H. and Lahiani, M., 2016. Study of the effects of human tissue on performance of a loop antenna. *IOSR J. Electr. Electron. Eng.*, *11*(4), pp.6-12.

[8] R. Das and H. Yoo, ''Application of a compact electromagnetic bandgap array in a phone case for suppression of mobile phone radiation exposure,'' *IEEE Trans. Microw. Theory Techn.*, vol. 66, no. 5, pp. 2363–2372, May 2018.

[9] X. Lin, B. Seet, F. Joseph, E. Li, "Flexible Fractal Electromagnetic Bandgap for Millimeter-Wave Wearable Antennas," in *IEEE Antennas Wirel. Propag. Lett.*, vol. 17, no. 7, pp. 1281–1285, Jul. 2018.

[10] Andreuccetti, D.; Fossi, R.; Petrucci, C. "An Internet Resource for the Calculation of the Dielectric Properties of Body Tissues in the Frequency Range 10 Hz–100 GHz," IFAC-CNR: Florence, Italy, 1997

[11] Lin, X., Seet, B.C., Joseph, F. and Li, E., 2018. Flexible fractal electromagnetic bandgap for millimeter-wave wearable antennas. *IEEE Antennas and Wireless Propagation Letters*, *17*(7), pp.1281-1285.

[12] Iqbal, A., Basir, A., Smida, A., Mallat, N.K., Elfergani, I., Rodriguez, J. and Kim, S., 2019. Electromagnetic bandgap backed millimeter-wave MIMO antenna for wearable applications. *IEEE Access*, *7*, pp.111135-111144.

[13] Ashraf, N., Haraz, O., Ashraf, M.A. and Alshebeili, S., 2015, May. 28/38-GHz dual-band millimeter wave SIW array antenna with EBG structures for 5G applications. In *2015 international conference on information and communication technology research (ICTRC)* (pp. 5-8). IEEE.

[14] L. Xu, L. Li and W. Zhang, "Study and Design of Broadband Bow-tie Slot Antenna Fed With Asymmetric CPW," in *IEEE Transactions on Antennas and Propagation*, vol. 63, no. 2, pp. 760-765, Feb. 2015, doi: 10.1109/TAP.2014.2378265.